V. Radchenko, D. V. Filosofov, O. K. Bochko, N. A. Lebedev, A. V. Rakhimov, H. Hauser,
M. Eisenhut, N. V. Aksenov, G. A. Bozhikov, B. Ponsard, and F. Roesch*

Separation of ^{90}Nb from zirconium target for application in *immuno*-PET

Abstract: Fast progressing *immuno*-PET asks to explore new radionuclides. One of the promising candidates is ^{90}Nb. It has a half-life of 14.6 h that allows visualizing and quantifying biological processes with medium and slow kinetics, such as tumor accumulation of antibodies and antibodies fragments or drug delivery systems and nanoparticles. ^{90}Nb exhibits a positron branching of 53% and an average kinetic energy of emitted positrons of $E_{mean} = 0.35$ MeV. Currently, radionuclide production routes and Nb^V labeling techniques are explored to turn this radionuclide into a useful imaging probe. However, efficient separation of ^{90}Nb from irradiated targets remains in challenge.

Ion exchange based separation of ^{90}Nb from zirconium targets was investigated in systems AG 1 × 8 – HCl/H_2O_2 and UTEVA-HCl. ^{95}Nb ($t_{1/2} = 35.0$ d), ^{95}Zr ($t_{1/2} = 64.0$ d) and ^{92m}Nb ($t_{1/2} = 10.15$ d) were chosen for studies on distribution coefficients. Separation after AG 1 × 8 anion exchange yields 99% of $^{90/95}$Nb. Subsequent use of a solid-phase extraction step on UTEVA resin further decontaminates $^{90/95}$Nb from traces of zirconium with yields 95% of $^{90/95}$Nb.

A semi-automated separation takes one hour to obtain an overall recovery of $^{90/95}$Nb of 90%. The amount of Zr was reduced by factor of 10^8. The selected separation provides rapid preparation (< 1 h) of high purity ^{90}Nb appropriate for the synthesis of ^{90}Nb-radiopharmaceuticals, relevant for purposes of *immuno*-PET. Applying the radioniobium obtained, $^{90/95}$Nb-labeling of a monoclonal antibody (rituximab) modified with desferrioxamine achieved labeling yields of > 90% after 1 h incubation at room temperature.

Keywords: Niobium-90, Niobium-95, Ion exchange, UTEVA, Monoclonal antibody, Desferrioxamine, Labeling.

---

*Corresponding Author: F. Roesch, Institute of Nuclear Chemistry, Johannes Gutenberg-University Mainz, Fritz-Strassmann-Weg 2, D-55128 Mainz, Germany, e-mail: frank.roesch@uni-mainz.de
V. Radchenko: Institute of Nuclear Chemistry, Johannes Gutenberg-University Mainz, Fritz-Strassmann-Weg 2, D-55128 Mainz, Germany
D. V. Filosofov, O. K. Bochko, N. A. Lebedev, A. V. Rakhimov: Dzhelepov Laboratory of Nuclear Problems, Joint Institute of Nuclear Research, Joliot-Curie 6, 141980, Dubna, Moscow region, Russian Federation
H. Hauser, M. Eisenhut: Radiopharmaceutical Chemistry, German Cancer Research Center, Im Neuenheimer Feld 280, D-69120 Heidelberg, Germany
N. V. Aksenov, G. A. Bozhikov: Flerov Laboratory of Nuclear Reactions, Joint Institute of Nuclear Research, Joliot-Curie 6, 141980, Dubna, Moscow region, Russian Federation
B. Ponsard: Institute of Nuclear Materials Science, BR2 Reactor, Radioisotopes and NTD Silicon Production, Belgian Nuclear Research Centre, SCKCEN, Boeretang 200, BE-2400 Mol, Belgium

1 Introduction

Molecular imaging plays a key role in tumour diagnosis as well as in evaluation of new drugs for tumour treatment [1, 2]. The advantage of molecular imaging techniques over more conventional readouts is that they can be performed *in vivo* with sufficient spatial and temporal resolution and high sensitivity and selectivity. In particular, positron emission tomography (PET) offers sensitivity with unlimited depth penetration imaging on a picomolar level of concentrations, which is not achievable by other techniques so far [3].

2-[^{18}F]fluoro-desoxy-D-glucose (FDG) is the most widely used tracer for PET imaging in oncology and has been extensively evaluated and established in clinical routine for initial staging, assessment of response to therapy, and diagnosis of recurrent disease in many tumors including lymphoma, non-small-cell lung cancer, head and neck cancer, and colorectal cancer. However, [^{18}F]FDG is not a specific tracer and *e.g.* not able to discriminate cancer or inflammation and infection. In addition, many tumours do not exhibit high metabolic rates and thus are not properly diagnosed with [^{18}F]FDG. Therefore, there is an urgent need for new PET-radiopharmaceuticals for the specific detection of cancer which address tumour specific targets. In this context antibodies are appropriate candidates [4].

Although a rather low number of all antibodies developed make it to a worldwide use in clinics, more than

20 antibodies are currently approved by the US Food and Drug Administration [5]. A variety of engineered monoclonal antibodies (mAb) and antibody fragments for difference targets of interest is currently under preclinical investigation [6–8]. *Immuno*-PET, which is tracking and quantifying of mAbs with PET, can be of great value in several stages of mAb development and application [9]. For faster pharmacokinetics, antibody fragments with lower size have been developed [10]. Their enhanced clearance dramatically reduces the interval between radiotracer injection and the actual imaging to hours instead of days. Positron-emitting radionuclides with medium-long half-lives of interest for the PET-imaging with antibody fragments are, for example, ^{64}Cu ($t_{1/2}$ = 12.7 h) [11–13], ^{86}Y ($t_{1/2}$ = 14.7 h) [14, 15], ^{76}Br ($t_{1/2}$ = 16.0 h) [16, 17].

Several crucial factors and characteristics apply to radionuclide candidates for *immuno*-PET. The most important ones are: i) a physical half-life paralleling the biological half-life of the mAb or antibody fragment; ii) a high positron branching with no or weak accompanying other radiation (β^-, γ) to offer high-sensitive PET imaging while reducing the radiation burden of the patient; iii) a preferably low β^+-energy to allow high-resolution PET imaging; and iv) the availability of the radionuclide, *i. e.* an efficient production and radiochemical separation route.

In previous reports we proposed ^{90}Nb as promising candidate for application in *immuno*-PET [18, 19]. Its intermediate half-life of 14.6 h and a high positron branching of 53% may make ^{90}Nb an ideal candidate for application with antibody fragments, monoclonal antibodies, drug delivery systems and nanoparticles. A recent work described efficient labeling of a proof-of-principle monoclonal antibody (rituximab) with ^{90}Nb [20]. The *in vitro* stability of the ^{90}Nb-Df-mAb was high. These promising results urge us to continue investigation on ^{90}Nb. In the present study an improved rapid separation strategy of ^{90}Nb from zirconium targets was developed. A reliable, fast and efficient separation process is mandatory to continue to investigate the preparation of ^{90}Nb-labeled monoclonal antibody on a more routine scale.

2 Materials and methods

2.1 Materials

Reagents where purchased from Sigma-Aldrich (Germany) and used without further purification unless otherwise stated. Deionized water (18 MΩ cm^{-1}) and ultra pure HCl solution were used. No further special measures were taken regarding working under strict metal-free conditions. The mAb rituximab (MabThera$^®$, 10 mg/mL) directed against CD20 was purchased from Roche Nederland BV (Woerden, The Netherlands). For purification of conjugated and labeled antibodies, PD-10 columns (GE Healthcare Life Science) were applied, for ion exchange chromatography resins AG 1 × 8 (200–400 mesh) (Bio-Rad, USA,) and DOWEX 50 × 8 (200–400 mesh) (BioRad, USA) were used and for solid extraction UTEVA (diamyl, amylphosphonate) resin (100–150 μm) (Triskem, France) was applied.

Distribution coefficients as well as the production yield, radionuclidic purity, radiochemical purity and separation yield of $^{90/95}$Nb were determined by γ-ray spectroscopy. The γ-ray spectroscopy was performed using an Ortec HPGe detector system and Canberra Genie 2000 software. The dead time of the detector was always kept below 10%. The detector was calibrated for efficiency at all positions with the certified standard solution QCY48, R6/50/38 (Amersham, UK).

The decontamination factor Zr/Nb was measured by inductively coupled plasma mass spectrometry (ICP-MS) and gamma-ray spectroscopy. ^{90}Nb-labeled N-suc-Df-mAb were analyzed by instant thin-layer chromatography (ITLC), and by high-performance liquid chromatography (HPLC) for radiolabeling efficiency and radiochemical purity. ITLC analyses of ^{90}Nb-labeled N-suc-Df-mAb was performed on chromatography strips (Biodex, NY). As mobile phase, 0.02 M citrate buffer (pH 5.0) was used. HPLC monitoring of the final products was performed on a Waters HPLC system using a BioSep-SEC-S 2000 size exclusion column (Phenomenex$^®$). As eluent, a mixture of 0.05 M sodium phosphate and 0.15 M sodium chloride (pH 6.8) solution was used at a flow rate of 0.5 mL/min.

2.2 Production of $^{90/92m/95}$Nb and ^{95}Zr isotopes

2.2.1 Radionuclides for measurement of distribution coefficients

For determination of distribution coefficients ^{92m}Nb ($t_{1/2}$ = 10.12 d) and ^{95}Zr ($t_{1/2}$ = 64.0 d) were applied.

For production of ^{92m}Nb, natural zirconium target foils (1.9 mg, 18 × 26 mm, 0.1 mm thickness) were irradiated for 1 h at the Phasotron facility at the Joint Institute of Nuclear Research (JINR), Dubna, Russian Federation, at 100 MeV proton energy and 3 μA current.

^{95}Zr was extracted from thorium metal target (1.2 g) irradiated at Phasotron facilities in JINR with protons energy 300 MeV and current 5 μA for 5 h.

Table 1: Main gamma emission energies of radionuclides used in this work [21].

Radionuclide	$t_{1/2}$ (days)	Main γ emission energies (keV)	Abundance (%)
^{92m}Nb	10.2	934.5	99.0
^{90}Nb	0.61	1129.0	82.0
^{95}Zr	64.0	724.2	44.2
		756.7	54.0
^{95}Nb	35.0	765.8	100.0

2.2.2 Radionuclides for development of separation strategies

To optimize a radioniobium/zirconium separation protocol, ^{90}Nb and ^{95}Nb were employed. ^{95}Nb was produced *via* the ^{94}Zr$(n, \gamma) \rightarrow {}^{95}Zr(\beta^{-}, t_{1/2} = 64\,\mathrm{d}) \rightarrow {}^{95}$Nb reactions from natural zirconium granules (1–3 mm, 99.8% ChemPur, Germany). Neutron irradiations were performed in the TRIGA reactor at the University of Mainz, Germany, and in the BR2 high-flux research reactor at the Belgian Nuclear Research Centre, Mol, Belgium. In the latter case (BR2), 404 mg of zirconium granules were irradiated in a thermal neutron flux of 3.5×10^{14} n cm^{-2} s^{-1} for 4 d to produce an activity of about 500 MBq of ^{95}Zr at end of irradiation.

^{90}Nb was produced *via* the ^{90}Zr$(p, n)^{90}$Nb reaction at the cyclotron MC32NI of the German Cancer Research Center Heidelberg. For irradiation, a stack of three discs of natural zirconium (natural abundance 51.45% ^{90}Zr) foils of 10 mm diameter and a thickness of 0.25 mm each were used. Irradiation was performed at 20 MeV proton energy and a current of 5 μA for 1 h. This initial proton energy was decreased by using an aluminum holder cover of 0.5 mm thickness to 17.5 MeV entering the 1st foil of Zr. At 24 h after end of irradiation (EOB), activities of $^{90/92m/95}$Nb and ^{95}Zr were measured by γ-ray spectroscopy and production yields and impurities were determined.

Main gamma lines of the radionuclides are listed in Table 1.

2.3 Determination of distribution coefficients and preliminary separation experiments

2.3.1 Preparation of stock solutions

^{92m}Nb was extracted from the irradiated zirconium target by anion exchange chromatography. In short, the zir-

conium target was placed into a plastic vial, and water (3 mL) and 28 M HF (1.5 mL) were added. For complete target dissolution an excess of conc. hydrofluoric acid (4 mL) was added. The mixture was loaded on a column filled with 500 mg of AG 1 × 8 resin, 200–400 mesh in F^{-} form. The column was washed with conc. HF (20 mL) and ^{92m}Nb was eluted with a mixture of 6 M HCl/1% H$_2$O$_2$ (2 mL).

The procedure for extraction of ^{95}Zr from irradiated thorium target was described in [22].

Finally, fractions contained ^{92m}Nb and ^{95}Zr were evaporated to dryness and dissolved in 6 M HCl (2 mL).

2.3.2 Preparation and conditioning of resins

For determination of distributions coefficients, the anion exchange resin AG 1 × 8, 200–400 mesh (4 g) was applied. The resin was first washed with water (10 mL), and then transferred to the Cl^{-} form *via* washing with 12 M HCl (20 mL). Finally, the resin was additionally washed with water (10 mL) to remove excess of Cl^{-}, and kept until drying for 48 h at room temperature.

The UTEVA resin was applied without further preconditioning.

2.3.3 Procedure for distribution coefficients determination

Distribution coefficients were determined by batch mode according to the following procedures: 50 mg of resin were placed in a 2 mL tube, then 1 mL of solution of appropriate concentrations of HF or HCl/H$_2$O$_2$ and 5 μL of the radionuclides stock solution were added. The mixture was vigorously stirred and allowed to stay for 24 h (4 h for mixtures contained hydrogen peroxide) at room temperature. Next, the mixtures were centrifuged and 900 μL of the solution was taken and measured by γ-ray spectroscopy. Distribution coefficient were calculated from equations (1), were $A_{50\,\mathrm{mg(res.)}}$ is the activity in 50 mg of the resin and $A_{50\,\mu\mathrm{L(sol.)}}$ is the activity in 50 μL of solution. Distribution coefficients have a dimension of cm^3/g.

$$K_{\mathrm{d}} = \frac{C_{\mathrm{phase1}}^{\mathrm{eq.}}}{C_{\mathrm{phase2}}^{\mathrm{eq.}}} = \frac{A_{1\,\mathrm{g(res.)}}}{A_{1\,\mathrm{mL(sol.)}}} = \frac{A_{50\,\mathrm{mg(res.)}}}{A_{50\,\mu\mathrm{L(sol.)}}} \quad \mathrm{cm}^3/\mathrm{g} \quad (1)$$

2.4 Preliminary separation experiments

The K_{d} values determined in the batch mode served for understanding of the principle behavior of Nb$^{\mathrm{V}}$ and Zr$^{\mathrm{IV}}$

on anion exchange resins and on UTEVA in hydrofluoric and mixed hydrochloric and peroxide media. In addition, dynamic experiments were conducted.

2.4.1 Separation of Zr^{IV} and Nb^{V} on anion exchange column

500 mg of pre-conditioned anion exchange resin in F^{-} from was placed in plastic column (1.5 × 7 cm). 260 mg of natural metallic zirconium spiked with ^{95}Zr and ^{92m}Nb was dissolved in 28 M hydrofluoric acid (5 mL) and passed through the column. The column was additionally washed with 28 M hydrofluoric acid (35 mL) to examine the breakthrough of Nb^{V}. Elution of niobium was performed later on by using of mixture 6 M HCl/2.44% H$_2$O$_2$. Fractions of 1 mL were collected.

2.4.2 Dependence of concentration of hydrogen peroxide on elution of Nb^{V}

The elution profile of Nb^{V} was examined in the presence of various hydrogen peroxide concentrations. A procedure similar to one described in the previous chapter was applied until the step of niobium elution. Then the column was washed with 6 M HCl (11 mL) and later with 6 M HCl/0.5% H$_2$O$_2$ (8 mL). Fractions of 1 mL were collected.

2.4.3 Separation of Zr^{IV} and Nb^{V} on UTEVA resin

The behavior of Zr^{IV} and Nb^{V} on UTEVA resin was evaluated in HCl media. Separation profiles for no-carrier-added ^{95}Zr^{IV} and ^{92m}Nb^{V} were measured for UTEVA (100–150 μm) in 4×75 mm columns in HCl. Aliquots from the stock solution were loaded on the column in 9 M HCl (1 mL) and next the column was consistently washed with 5.5 M HCl (3 mL), 4.5 M HCl (3 mL) and 2 M HCl (6 mL).

2.5 Separation strategy

2.5.1 Target dissolution

The irradiated zirconium target, typically (260×3 mg), was placed into a 15 mL plastic vial and water (500 μL) was added. For dissolution, 28 M hydrofluoric acid (500 μL) was portionally added and after full dissolution concentrated hydrofluoric acid (1 mL) was added.

2.5.2 Crude separation

Based on the distribution coefficients and preliminary separations, the following separation strategy was established.

2 mL of 21 M hydrofluoric acid containing the irradiated zirconium target were passed through the cation exchange column (DOWEX 50×8 resin, 200–400 mesh, 10×5 mm, 100 mg) resin in F^{-} form for removal of colloids, unsolved target particles and possible trace contamination of 2+ and 3+ charged metal cations, which may originate from target impurities. The column was additionally washed with concentrated hydrofluoric acid (1 mL). The solution (3 mL) which passed the cation exchange resin was transferred to an anion exchange column (300 mg, 25x5 mm) filled with AG 1 × 8 resin (200–400 mesh) resin in F^{-} form. Nb^{V} remained on this resin and the bulk amount of Zr^{IV} passed through. The column was washed with concentrated HF (4.5 mL) to elute traces of Zr^{IV}, while $^{90/95}$Nb stays on the column. To completely remove traces of hydrofluoric acid prior to elution of Nb^{V}, the column was washed with 1 M HCl (1 mL). Next 6 M HCl/1% H$_2$O$_2$ (500 μL) were passed through the column and collected. Finally, $^{90/95}$Nb was eluted with another 500 μL of the same mixture. To remove the hydrogen peroxide, this $^{90/95}$Nb fraction was heated for 5 min at 120 °C.

2.5.3 Final purification of $^{90/95}$Nb on UTEVA resin

A small column (100 mg, 10 × 5 mm) was filled with UTEVA resin. To 6 M HCl (700 μL) fraction containing $^{90/95}$Nb, 12 M HCl (700 μL) were added. This 1.4 mL of solution was passed through the UTEVA which was next washed with 5 M HCl (5 mL). Traces of zirconiumIV, and Nb^{V} remain absorbed on the column. For elution of $^{90/95}$Nb 1 M oxalic acid was applied. The column was washed with 200 μL and Nb eluted with another 400 μL of 1 M oxalic acid. The decontamination factor Zr/Nb was measured by inductively coupled plasma mass spectrometry (ICP-MS) and γ-ray spectroscopy.

2.5.4 Development of a semi-automated module

The manually performed process takes about 1.5–2 h. To shorten the separation time, a semi-automated module was developed, *cf*. Figure 1.

The transfer of solutions is carried out under pressure of argon (99.996 vol.%, Westfalen AG, Germany). All parts of the module were made from resistant to hydroflu-
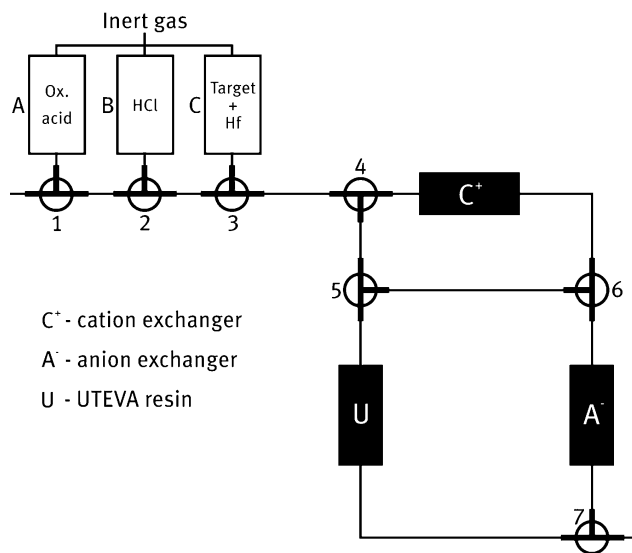
Fig. 1: Schematic view of semi-automated separation module.

oric acid materials (polyethylene, polyether ether ketone (PEEK), teflon).

The irradiated zirconium target was placed into vial C with addition of water (500 μL). Hydrofluoric acid (500 μL) was added portionally trough the tube, and after full target dissolution 1 mL HF was added. The two milliliters were passed through the cation and anion exchange columns (valves 3, 4 and 6). To vial C another 1 mL of hydrofluoric acid was added to pass by the same way. Subsequently, 4.5 mL of 28 M HF was passed through the anion exchange column (valves 4, 5 and 6). The anion exchange column was washed with 1 M HCl (1 mL) from vial B (valves 2 and 3). ^{95}Nb was eluted from the anion exchanger with a mixture of 6 M HCl/1% H_2O_2. The first 500 μL were passed through and another 700 μL contained $^{90/95}$Nb. After 5 min heating at 120 °C another 700 μL of 12 M HCl were added. The mixture was loaded in vial B and passed through the UTEVA resin (valves 5 and 7). In vial B 5 M HCl (5 mL) was loaded and passed through the UTEVA resin. Finally, 1 M oxalic acid from vial
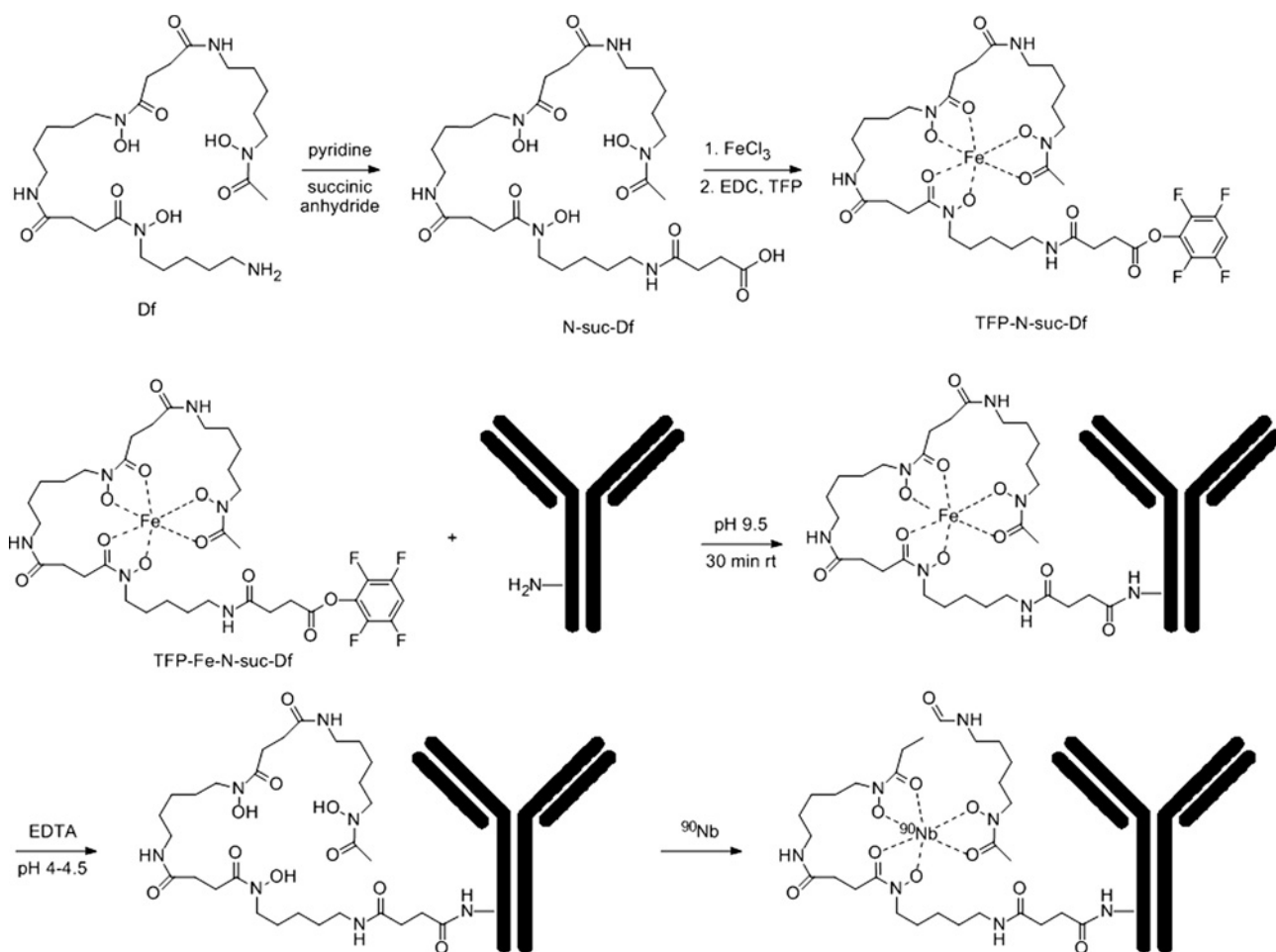

Fig. 2: Df-conjugation *via* TFP-N-suc-Df-Fe and labeling with ^{90}Nb.

A, was applied to elute [90/95]Nb. The first 200 μL of oxalic acid were passed through the UTEVA resin (valves 1 and 2) and [90/95]Nb was eluted with the following 400 μL into an external product vial.

2.6 Preparation of [90]Nb-labeled N-suc-Df-rituximab

To demonstrate the potential of [90/95]Nb separated as described, the Df-conjugated monoclonal antibody N-suc-Df-rituximab [23], Figure 2, was labeled with [90/95]Nb in HEPES buffer at pH 7.0. The labeling procedure was similar to a previously developed protocol reported in [20]. In short, to 200 μL [90/95]Nb (37 MBq for [90]Nb) in 1 M oxalic acid a solution of 2 M Na_2CO_3 (90 μL) was added and the mixture was allowed to stay for 3 min. Next, 0.5 M HEPES buffer (300 μL) pH 7.2 and N-suc-Df-mAb (250 μg) were added. Finally, 0.5 M HEPES buffer (700 μL) were added. The overall volume of the reaction mixture was 2 mL. The mixture was incubated for 1 h at room temperature. At various time point's kinetics was monitored by thin layer chromatography (TLC) and high pressure liquid chromatography (HPLC). After 1 h [90/95]Nb-N-suc-Df-mAb was purified on a PD-10 column using 0.9% sodium chloride solution as mobile phase.

3 Results

3.1 Production of niobium and zirconium isotopes

[92m]Nb: Two weeks after irradiation, the isotopic content of the irradiated zirconium target was evaluated by γ-ray spectroscopy. At this time point, the activity of [92m]Nb ($t_{1/2}$ = 10.15 d) was 2.5 MBq. Radiochemical separation recovered more than 90% of [92m]Nb.

[95]Zr/[95]Nb: More than 500 MBq of [95]Zr was produced at the BR2 reactor after 4 days of irradiation in a thermal neutron flux of 3.5×10^{14} n cm^{-2} s^{-1}. The maximum daughter activity of [95]Nb as generated from [95]Zr was obtained at ~ 67 d after EOB.

[90]Nb: The overall [90]Zr(p, n) irradiation yield of [90]Nb for 1 h and 5 μA irradiations was 720 ± 50 MBq, *i. e.* 145 ± 10 MBq/μAh under the given irradiation parameters. The isotopic purity of [90]Nb after EOB was more than 97%. Minor isotopic impurities found were: [92m]Nb = 1.64%, [95]Nb = 0.08%, [95m]Nb ($t_{1/2}$ 3.6 d) = 0.29% and [96]Nb ($t_{1/2}$ 23.35 h) = 0.88%.

3.2 Determination of distribution coefficients

Distribution coefficients to understanding the behaviour of Zr[IV] and Nb[V] on anion exchange resin and UTEVA in HCl/H_2O_2 media in a static system are shown in Figs. 3, 4 and 5 respectively.

However, determination of K_d values in HCl/H_2O_2 were accompanied with some complicity. Incubation time is needed to setup equilibrium between tracers, resin and media, but this equilibrium is disturbed because hydrochloric acid reacts with hydrogen peroxide and with time changes its concentration. Therefore 4 hours was found to be an optimum incubation period for equilibrium and for low concentration changes. Errors in samples with-
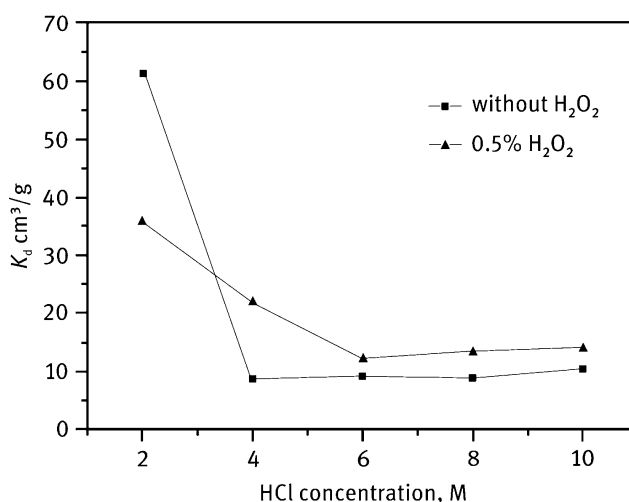

Fig. 3: K_d values for Nb[V] in the system AG 1 × 8 (200−400 mesh) − HCl.
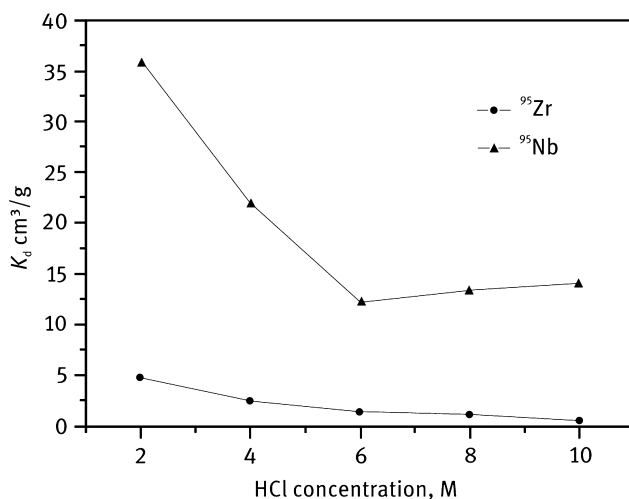

Fig. 4: K_d values for Zr[IV] and Nb[V] in system AG 1 × 8 (200−400 mesh) − HCl − 0.5% H_2O_2.
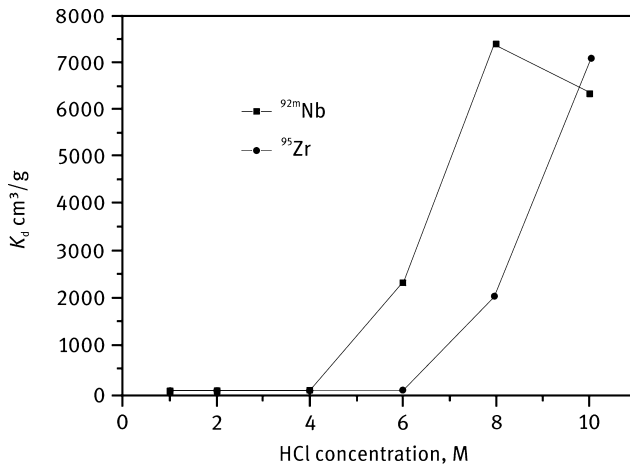
Fig. 5: K_d values for Zr^{IV} and Nb^V in the system UTEVA – HCl.

out hydrogen peroxide were below 10% and in presence of hydrogen peroxide up to 30%.

3.2.1 Zr^{IV} and Nb^V distribution coefficients in the system AG 1×8 – HCl/H$_2$O$_2$

Distribution coefficients in various hydrochloric acid concentrations and mixtures of HCl and hydrogen peroxide are illustrated in Figure 3 for the anion exchange process.

Significant differences in presence of hydrogen peroxide were not observed. However, K_d values are slightly higher with H$_2$O$_2$. With increasing concentration of hydrochloric acid, distribution coefficients decrease especially at HCl concentrations (between 2 and 4 M). From 6–10 M HCl differences are insignificant. Such relation is in good agreement with previous data [25].

Slightly different behaviour of Zr^{IV} and Nb^V in presence of 0.5% peroxide was observed. K_d values for Zr^{IV} are lower than for Nb^V, and maximal differences can be seen at low HCl concentrations (0–4 M) (Figure 4). This represents an advantageous option for additional decontamination of niobium from zirconium.

3.2.2 Zr^{IV} and Nb^V distribution coefficients in the system UTEVA-HCl

Studies on sorption of zirconium and niobium on UTEVA resin in hydrochloric acid are shown in Figure 5.

At low HCl concentration, Zr^{IV} and Nb^V show a similar distribution. However, with increasing concentration of hydrochloric acid significant differences in K_d appear. Between 6 and 8 M HCl, K_d values are much higher for Nb^V.

3.3 Preliminary separation experiments

To transfer data on distribution coefficients from static condition to "real" situations, several preliminary separation experiments were conducted to determine optimal parameters for a final separation procedure.

3.3.1 Separation of Zr^{IV} and Nb^V on anion exchange column

The separation profile of Zr^{IV} and Nb^V (Figure 6) allow a crude separation of radioniobium from bulk amounts of zirconium.

The first fraction (40 mL) contained > 99% of the ^{95}Zr while no breakthrough of Nb^V was measured. Subsequent washing the column with a mixture of 6 M HCl/2.44% H$_2$O$_2$ elutes ^{92m}Nb. Most of its activity ($\geq$ 99%) was found in fractions 5–7 (3 mL), with no activity of ^{95}Zr detected.

3.3.2 Effect of H$_2$O$_2$ on the elution of Nb^V

Despite the K_d values which did not show sufficient differences in presence of hydrogen peroxide and without, there is a significant effect when eluting ^{92m}Nb from the anion exchange column. 6 M HCl elutes radioniobium as broad peak (fractions f10–f20, 10 mL) and allows eluting $\leq$ 50% of the ^{92m}Nb activity. However, after applying a mixture of 6 M HCl/0.5% H$_2$O$_2$ from fraction f21, the remaining ^{92m}Nb was eluted in 1.5 mL of that mixture (Figure 7). Such disagreement between column separation and distri-
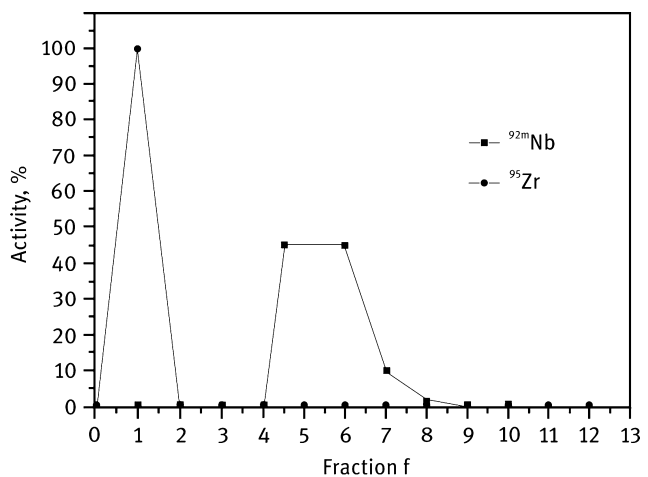

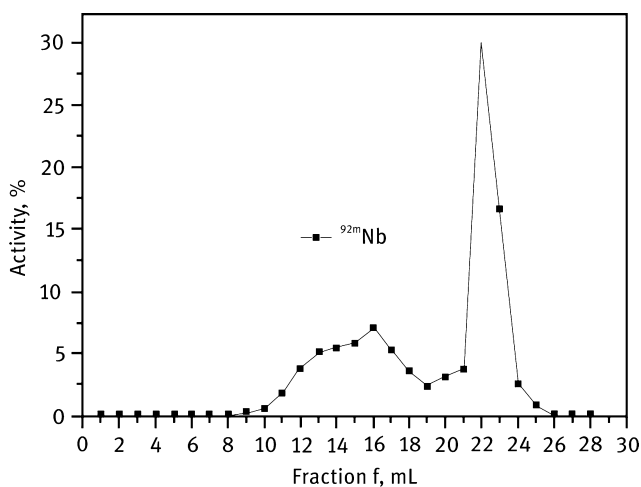**Fig. 6:** Separation profile of Zr^{IV} and Nb^V on anion exchange column in hydrofluoric media.

Fig. 7: Elution profile of Nb^V from anion exchange column in HCl/H$_2$O$_2$.
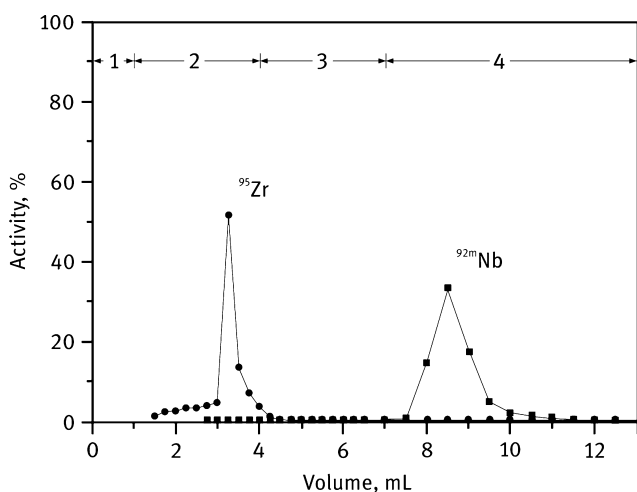

Fig. 8: Elution profile of Zr^{IV} and Nb^V from UTEVA column (4 × 75 mm) with various HCl concentrations: 1 – 9 M HCl, 2 – 5.5 M HCl, 3 – 4.5 M HCl, 4 – 2 M HCl.

bution coefficients can be explained by the phase contact time.

3.3.3 Separation of Zr^{IV} and Nb^V on UTEVA resin

Based on distribution coefficients, a preliminary separation was tested with no-carrier-added Zr^{IV} and Nb^V on UTEVA resin in various concentrations of HCl. The most effective separation was achieved with HCl (Figure 8). Elution of Zr^{IV} at 5.5 M HCl was almost quantitative ($\geq$ 99%), Nb^V was eluted completely with of 2 M HCl (4 mL).

3.4 Final separation strategy

The overall separation proceeds with a separation yield of more than 99% of $^{90/95}$Nb after anion exchange. The final fraction of 1 M oxalic acid (400 μL) contains more than 95% of $^{90/95}$Nb. The whole separation procedure takes around 1.5 h, which is almost 4 times faster than the previous separation method [19]. The decontamination factor for Zr after anion exchange was 1×10^5 and after UTEVA purification 3×10^8. This decontamination factor equals 0.77 ng of zirconium presented in final fraction for a 260 mg zirconium target.

This procedure was adapted to a semi-automated separation module. The separation yield of $^{95/90}$Nb in the final fraction was somewhat lower (90%) what can be explained by losses on valves and tubes during the separation procedure. However, this takes even shorter time (1 h) and allows remote operation that is very important factor in case of high activity irradiations.

3.5 Proof-of-principle labeling of N-suc-Df-rituximab

The $^{90/95}$Nb labeling kinetics indicate that the radiochemical yield reached 60% already after 15 min and increased to more than 90% after 50 min (95% analyzed by instant thin layer chromatography (ITLC) and 93% by size exclusion chromatography (SEC)). After SEC separation on a PD-10 column, the $^{90/95}$Nb-Df-mAb was of 99.0% purity.

4 Discussions

Our aim was to develop an improved separation protocol. Isolation of ^{90}Nb should be fast, effective and less complicated compared to known protocols. It should provide a reliable source of ^{90}Nb with appropriate properties for following labelling reactions.

Previously reported work indicates effective separation of Zr^{IV} and Nb^V in mixed hydrofluoric acid media on anion exchange resins [26]. Fluoro complexes of niobium are well studied. Therefore we initially designed our new separation strategy on the very different behaviour of Zr^{IV} and Nb^V in hydrofluoric acid media. Due to future application of ^{90}Nb for medical purposes, however, the absence of traces of hydrofluoric acid in the final product is obligatory. Therefore we decided to prefer a two-step separation procedure, where the first step allows crude removal of the target material, followed by a second step for addi-

tional purification and conditioning for following medical application.

Compared to previous separation methods [19], including multistep separations by liquid-liquid extraction and anion exchange, the alternative separation strategy developed is: i) decreased separation time by a factor of four (from 4 to 1 h); ii) increased separation yield to 90%–95% (instead of 76%–81% for previous strategy); iii) 10 fold improved decontamination factor for Zr/Nb ($> 10^8$), that will allow preparation of radiopharmaceuticals with higher specific activity (in case of a standard target setup, just 0.77 ng of Zr will be presented in final fraction); and iv) designed and tested in a semi-automated separation module for remote separation.

The final elution of Nb^V in 1 M oxalic acid allows keeping radio-Nb in an appropriate species for subsequent labeling and prevents possible hydrolyzation. The $^{90/95}$Nb fraction obtained is adequate to subsequent radiolabeling.

The purified $^{90/95}$Nb proved excellent labelling of a N-suc-Df conjugated for purposes of *immuno*-PET. Thus developed separation strategy provides a reliable source of ^{90}Nb for application in *immuno*-PET.

References

1. Willmann, J. K., van Bruggen, N., Dinkelborg, L. M., Gambhir, S. S.: Molecular imaging in drug development Nature Rev. Drug Disc. **7**, 591 (2008).
2. Ottobrini, L., Ciana, P., Biserni, A., Lucignani, G., Maggi, A: Molecular imaging: a new way to study molecular processes *in vivo*. Mol. Cell Endocrinol. **246**(1–2), 69 (2006).
3. Czernin, J., Weber, W. A., Herschman, H. R.: Molecular imaging in the development of cancer therapeutics. Annu. Rev. Med. **57**, 99 (2006).
4. Wu, A. M., Olafsen, T.: Antibodies for molecular imaging of cancer. Cancer, J. **14**, 191 (2008).
5. U. S. Food and Drug Administration, U. S. Department of Health and Human Services. [Website] 2010, Available, from http://www.fda.gov.
6. Carter, P. J.: Potent antibody therapeutics by design. Nature Rev. Immunol. **6**, 343 (2006).
7. Reichert, M. J., Rosensweig, C. J., Faden, L. B., Dewitz, M. C.: Monoclonal antibody successes in the clinic. Nature Biotechnology **23**, 1073 (2005).
8. Mould, D. R., Sweeney, K. R. D.: The pharmacokinetics and pharmacodynamics of monoclonal antibodies – mechanistic modeling applied to drug development. Cur. Opinion in drug disc. Dev. **10** (1), 84 (2007).
9. van Dongen, G. A. M. S., Vosjan, M. J. W. D.: Immuno-Positron Emission Tomography: Shedding Light on Clinical Antibody Therapy. Canc. Biother. & Radiopharm. **25**(4), 375 (2010).
10. Boder, E. T., Jiang, W.: Engineering Antibodies for Cancer Therapy. Ann. Rev. Chem. and Biomol. Engin. **2**(1), 53 (2011).
11. Paudyal, B., Paudyal, P., Oriuchi, N., Hanaoka, H., Tominaga, H., Endo, K.: Positron emission tomography imaging and biodistribution of vascular endothelial growth factor with

^{64}Cu-labeled bevacizumab in colorectal cancer xenografts. Cancer. Science. **102**(1), 117 (2011).
12. Zhou, Y., Liu, S.: ^{64}Cu-labeled phosphonium cations as PET radiotracers for tumor imaging. Bioconjug. Chem. **22**(8), 1459 (2011).
13. Di Bartolo, N., Sargeson, A. M., Smith, S. V.: New ^{64}Cu PET imaging agents for personalised medicine and drug development using the hexa-aza cage, SarAr. Org. Biomol. Chem. **4**(17), 3350 (2006).
14. Herzog, H., Rösch, F., Stöcklin, G., Lueders, C., Qaim, S. M., Feinendegen, L. E.: Measurement of pharmacokinetics of yttrium-86 radiopharmaceuticals with PET and radiation dose calculation of analogous yttrium-90 radiotherapeutics. J. Nucl. Med. **34**, 2222 (1993).
15. Nayak, T. K., Garmestani, K., Baidoo, K. E., Milenic, D. E., Brechbiel, M. W.: PET imaging of tumor angiogenesis in mice with VEGF-A-targeted (86)Y-CHX-A?-DTPA-bevacizumab. Int. J. Cancer. **128**(4), 920 (2011).
16. Rossin, R., Berndorff, D., Friebe, M., Dinkelborg, L. M., Welch, M. J.: Small-animal PET of tumor angiogenesis using a ^{76}Br-labeled human recombinant antibody fragment to the ED-B domain of fibronectin. J. Nucl. Med. **48**, 1172 (2007).
17. Watanabe, S., Hanaoka, H., Liang, J. X., Iida, Y., Endo, K., Ishioka, N. S.: PET imaging of norepinephrine transporter-expressing tumors using ^{76}Br-meta-bromobenzylguanidine. J. Nucl. Med. **51**(9), 1472 (2010).
18. Busse, S., Rösch, F., Qaim, S. M.: Cross section data for the production of the positron emitting niobium isotope ^{90}Nb *via* the ^{90}Zr(p, n)-reaction. Radiochim. Acta **90**, 1 (2002).
19. Busse, S., Brockmann, J., Roesch, F.: Radiochemical separation of no-carrier-added radioniobium from zirconium targets for

application of ^{90}Nb-labelled compounds. Radiochim. Acta **90**, 411 (2002).

20. Radchenko, V., Hauser, H., Eisenhut, M., Vugts, J. D., van Dongen, G. A. M. S., Roesch, F.: ^{90}Nb – a Potential PET Nuclide: Production and Labeling of Monoclonal Antibodies. Radiochim. Acta **100**(11), 857 (2012).

21. Browne, E., Firestone, R. B.: *Table of Radioactive Isotopes*, (Shirley, V. S. ed.) John Wiley and Son, New York (1986).

22. Filosovof, D. V., Bojikov, G. A., Sadiikov, I. I., Karaivanov, D. V., Lebedev, N. A., Norseev, Yu. V., Rakhimov, A. V.: Extraction of various radionuclides from Th target irradiated by 300 MeV protons. submitted to Radiochimya (2013).

23. Verel, I., Visser, G. W. M., Boellaard, R., van Walsum, S. M., Snow, G. B., van Dongen, G. A. M. S. ^{89}Zr *immuno*-PET: comprehensive procedures for the production of ^{89}Zr-labeled monoclonal antibodies. J. Nucl. Med. **44**, 1271 (2003).

24. Vosjan, M. J. W. D., Perk, L. R., Visser, G. V. M., Budde, M., Jurek, P., Kiefer, G. E., van Dongen, G. A. M. S.: Conjugation and radiolabeling of monoclonal antibodies with zirconium-89 for PET imaging using the bifunctional chelate *p*-isothiocyanatobenzyl-desferrioxamine. Nature. Protocols **5**(4), 739 (2010).

25. Marchol, M. *Ion Exchangers in Analytical chemistry: Their Properties and Use in Inorganic Chemistry.* Volume 2, Prague, Czech Republic: Academia, 1982.

26. Fassbender, M., Jamriska, D. J., Hamilton, V. T., Nortier, F. M., Phillips, D. R., Simultaneous ^{68}Ge and ^{88}Zr recovery from proton irradiated Ga/Nb capsules (LA-UR #03-2319), Journal of Radioanalytical and Nuclear Chemistry **263**(2), 497–502 (2003).